Contents lists available at ScienceDirect

Food Hydrocolloids

Characteristics and application of fish oil-in-water pickering emulsions structured with tea water-insoluble proteins/κ-carrageenan complexes

Zhongyang Ren [a,b], Zhanming Li [c,d], Zhongzheng Chen [b], Yuanyuan Zhang [b], Xiaorong Lin [b], Wuyin Weng [a], Hongshun Yang [c,*], Bin Li [b,**]

[a] College of Food and Biological Engineering, Jimei University, Xiamen, 361021, China
[b] College of Food Science, South China Agricultural University, 483 Wushan Street, Tianhe District, Guangzhou, 510642, China
[c] Department of Food Science & Technology, National University of Singapore, Science Drive 2, Singapore, 117542, Singapore
[d] School of Grain Science and Technology, Jiangsu University of Science and Technology, Zhenjiang, 212004, China

ABSTRACT

Food-grade Pickering emulsions (PEs) stabilized by proteins and polysaccharides have enormous application potential for preparing oil gels. Tea water-insoluble protein (TWIP) and κ-carrageenan (KC) were applied to prepare fish oil-in-water PEs and fish oil gels to broaden the application of fish oils at different ratios of TWIPs and KC. The turbidity reduced, but particle size unchanged except that of TWIP/KC mixture at 80:20 and zeta potential was not altered with the addition of KC. The β-turn and random coil of TWIPs were transformed into β-sheet, α-helix and β-antiparallel due to the addition of KC. Besides, TWIPs clustered with the increase of KC content, especially at 80:20. The droplets of the PEs stabilized by TWIP/KC mixtures were relatively small and homogeneous and the viscoelastic behavior of them was improved compared with those stabilized by TWIPs only. Finally, fish oil gels prepared using PEs stabilized by TWIP/KC mixtures had solid-like behavior with a storage modulus of almost 200 kPa. Therefore, TWIP/KC mixtures can be applied to prepare stable PEs and fish oil gels utilizing PEs as templates. These findings will help explore new edible materials, construct novel colloid structures of underused edible materials and their eventual use in real food manufacture.

1. Introduction

Pickering emulsions (PEs) stabilized by solid particles, rather than small molecular weight surfactants, have been mentioned for more than 100 years; however, PEs, especially those stabilized by food-grade materials, have received insufficient attention the last 30 years (Berton-Carabin, Sagis, & Schroën, 2018; Xiao, Li, & Huang, 2016). Using food-grade particles to structure PEs has attracted the interest of food researchers because of their potential application in food materials (Jiang et al., 2019; Liu & Tang, 2016; Wang et al., 2016; Wei, Yu, et al., 2020). These particles are very stable and almost irreversibly adsorbed at the oil-water interface compared with surfactants; therefore, PEs stabilized using food-grade particles exhibit satisfactory storage stability in comparison with traditional emulsions stabilized by surfactants (Wei, Tong, et al., 2020; Wei et al., 2019; Zhou et al., 2019).

Recently, extensive studies of PEs have concentrated on the food-grade particles. PEs can be structured by polysaccharides and proteins

(Marefati, Bertrand, Sjöö, Dejmek, & Rayner, 2017; Xiao et al., 2016). Some complexes are also used to prepare PEs to improve their gel-like behaviors such as zein/pectin complexes (Jiang et al., 2019). The use of SPI and κ-carrageenan (KC) complexes can lead to better long-term stability of emulsions compared with the use of SPI alone; meanwhile, oil gels obtained after removing water from the SPI/KC stabilized emulsions have a good gel strength with the increase in KC content due to the formation of the thick interface (Tavernier, Patel, Van der Meeren, & Dewettinck, 2017). The strong gelation potential of KC might be beneficial for delivery systems prepared by proteins since KC can stabilize some proteins to create a stable gel state compared with protein-only gels (Selig et al., 2018).

According to previous reports, tea water-insoluble proteins (TWIPs), derived from tea byproducts, possess good emulsifying properties and amphipathic property (Ren, Chen, Zhang, Zhao, et al., 2019). TWIPs are the main component in tea residues, which can be used to prepare PEs via high-speed homogenization (Ren, Chen, Zhang, Lin, & Li, 2019). In

addition, PEs stabilized by TWIPs at a soy oil-water ratio of 6:4 (v/v) and a TWIP concentration of 4.0% (v/v), prepared using the high-pressure homogenization, possess good storage stability and gel-like behavior (Ren, Chen, Zhang, Lin, & Li, 2020). However, their gel-like behavior is not strong enough to broaden their application in food colloidal systems. To improve the gel-like behavior of food-grade emulsions, polysaccharides are usually added such as pectin and KC (Mao, Wang, Tai, Yuan, & Gao, 2017; Sow, Chong, Xu, & Yang, 2018; Sow, Kong, & Yang, 2018; Tavernier et al., 2017). KC from red seaweed is negatively charged that has good biocompatibility and is abundant in nature (Sow, Chong, et al., 2018). Emulsions prepared with SPI/KC complexes can form a thick interfacial layer and show much strong viscoelastic behavior (Tavernier et al., 2017). However, the effect of KC on the characteristics of PEs stabilized by TWIP/KC mixtures is unknown.

Lipids in foods like margarine and shortenings contain large amounts of trans/saturated fatty acids (Tavernier, Heyman, Van der Meeren, Ruyssen, & Dewettinck, 2019). These trans/saturated fatty acids have an adverse effect on the health of consumers like cardiovascular diseases and even some countries legislate for trans fatty acids to limit the usage of these fatty acids (Souza et al., 2015). By contrast, the consumption of polyunsaturated fatty acids could prevent coronary heart diseases (Endo & Arita, 2016). Fish oils contain lots of polyunsaturated fatty acids, especially n-3 eicosapentaenoic acid (EPA) and docosahexaenoic acid (DHA), which can enhance the cardiovascular and immune systems (Chang et al., 2018). However, these polyunsaturated fatty acids are easily degraded to produce oxidized products. PEs can inhibit oil oxidation to enhance oxidative barrier properties (Linke & Drusch, 2018). Freeze-drying has been applied to prepare semisolid fats containing few saturated/trans fats (Gao et al., 2014). Protein-based oil gels can be used for the reduction of saturated fats and the delivery of proteins in lipid-based foods (Patel, 2018).

Therefore, this study aimed to explore the characteristics and application of fish oil-in-water PEs stabilized using TWIP/KC mixtures at a mixture concentration of 4.0% (w/v) and a fish oil-water ratio of 6:4 (v/v). First, the characteristics of the TWIP/KC mixtures were analyzed via particle size and zeta potential analyzer, atomic force microscopy (AFM) and Fourier transform infrared (FTIR) spectroscopy. Furthermore, PEs stabilized using TWIP/KC mixtures and fish oil gels were characterized.

2. Materials and methods

2.1. Materials

TWIPs were prepared in South China Agricultural University (Guangzhou, Guangdong, China). The KC was provided by the FMC company (Philadelphia, PA, USA). KBr and Nile blue A were purchased from Merck KGaA (Darmstadt, Germany). Fish oils from Menhaden fish (*Clupea pallasi*) were obtained from Sigma-Aldrich, Inc (St. Louis, MO, USA). All solutions and dispersions were prepared using deionized water.

2.2. Preparation of fish oil-in-water emulsions and oil gels

TWIPs were hydrated at 4 °C for 24 h. The solution was then adjusted to pH 7.0. KC and added to the TWIP solution according to the ratio of TWIPs and KC (w/w), with stirring for 2 h, at the solid concentration of 4.0% (w/v) according to Table S1 referred to previous reports (Ren, Chen, Zhang, Lin, et al., 2019). The concentration of KC was limited to no more than 0.80% (w/v) to avoid over modify TWIP and form gels before emulsification. The pH of the mixtures was then determined. Liquid samples were prepared for further analysis.

Emulsions were prepared at a fish oil and TWIP/KC solution ratio of 6:4 (v/v) following a previously published method with slight changes (Li, Zeng, et al., 2020). In brief, the TWIP/KC solution (20 mL) was homogenized with fish oils (30 mL) at 20,000 rpm for 2 min using an emulsifying machine (SUOTN, 50 CE0S–H, Shanghai, China) and further treated using an ultrasonic processor (Scientz, JY92-IIN, Ningbo, China) at 384 W for 4 min (5 s ON and 5 s OFF). To obtain the fish oil gels, emulsion samples were dried using vacuum-freeze drying for 48 h. Emulsions and oil gel samples were tightly sealed and stored at 4 °C for subsequent testing. The oil gels were mixed uniformly before the tests.

2.3. Measurement of turbidity, particle size, and zeta potential of TWIP/KC mixtures

The absorbance of the samples was tested at 25 °C using an ultraviolet–visible spectrophotometer at 600 nm (Shimadzu, UV-1700, Kyoto, Japan). The turbidity (τ) was determined using Eq. (1) (Sow, Chong, et al., 2018).

$$\tau = -(1/L)ln(I/I_0) = A/L \tag{1}$$

where L, I and I_0 are the optical path (cm), transmitted radiation intensity and incident radiation intensity, respectively.

Liquid samples were diluted 100 times before testing. The hydrodynamic diameter (D_H) and zeta potential of samples were analyzed using particle size and zeta potential analyzer (Brookhaven, NanoBrook 90 Plus Zeta, NY, USA).

2.4. Atomic force microscopy (AFM)

TWIP/KC mixtures were tested in the tapping mode using AFM (AFM workshop, Signal Hill, CA, USA) according to a previous method (Zhou & Yang, 2019). The sample solution was diluted to 2 μg/mL, dropped on a cleaved mica surface and dried overnight. The number of scan lines and the rate were 512 and 0.4 Hz, respectively. Gwyddion 2.53 software was used to analyze the different regions in the AFM images (15 μm × 15 μm) (Nečas & Klapetek, 2012).

2.5. FTIR spectroscopy

Samples were analyzed by the FTIR spectrometer (Vertex 70, Bruker Daltonics, Hamburg, Germany) according to the previous method (Sow, Tan, & Yang, 2019). The FTIR spectra were scanned 64 times at a wavenumber of 4000–500 cm^{-1} and a resolution of 4 cm^{-1}. The spectra of amide I (1700-1600 cm^{-1}) were processed using Origin Pro 9.0.5 (OriginLab, Northampton, MA, USA). The secondary structure of the samples was quantified according to their peak areas.

2.6. Wettability measurement

The oil-in-water contact angle (θo/w) of TWIP/KC mixtures was determined with an SDC 200 (SINDIN Precision Instrument, China) by a previous method with some changes (Wei, Yu, et al., 2020). The TWIP/KC mixtures were compressed to a tablet with a thickness of 2 mm and a diameter of 10 mm. The tablets were put into fish oils in a quartz cell. A droplet of 2 μL was dropped on the surface of the tablets. The contact angle was acquired using the circle method.

2.7. Characterization of PEs and fish oil gels

2.7.1. Measurements of droplet size and droplet size distribution

The droplet size and droplet size distribution of the emulsions were obtained using a laser diffraction particle sizing instrument (LA950, Horiba, Japan) according to a previous method (Akamatsu, Kanasugi, Nakao, & Weitz, 2015). The procedure comprised cleaning the system, debubbling, rinsing and adding the samples to test. The refractive index of water was 1.33 and deionized water was used as the dispersant. The area-average diameter ($d_{3,2}$, μm) and volume-average diameter ($d_{4,3}$, μm) of the droplets were evaluated following Eq. (2) and Eq. (3), respectively.

$$d_{3,2} = \sum n_i d_i^3 \Big/ \sum n_i d_i^2 \qquad (2)$$

$$d_{4,3} = \sum n_i d_i^4 \Big/ \sum n_i d_i^3 \qquad (3)$$

where n_i is the number of droplets of PEs stabilized by TWIP/KC mixtures in water with diameter d_i.

2.7.2. Rheology measurement

The rheological properties of the TWIP/KC mixtures-stabilized PEs and fish oil gels were determined using a controlled-stress rheometer (MCR 102, Anton Paar, Graz, Austria) with an intelligentized Tool-Master and sample adaptive controller TruRate™ (Anton Paar) according to a previous report (Sow, Kong, et al., 2018). The apparent viscosity was analyzed at shear rates of $0.1-100 \text{ s}^{-1}$. The diameter of the parallel plate was 50 mm. The gap was set as 1 mm. A frequency sweep under the linear viscoelastic region was performed at $0.1-100$ rad/s and a shear strain of 0.5%. The gap was fixed at 1 mm. All the tests were performed at 25 ± 0.1 °C. The storage modulus (G′) and loss modulus (G″) were recorded.

2.8. Fluorescent microscopy

Emulsions were stained with 1 mg/mL Nile Blue A. The stained PEs stabilized by TWIP/KC mixtures were dropped onto slides for observation. An argon laser was used to excite the fluorescence of Nile blue A at 488 nm under a fluorescent microscope (Olympus, BX51, Tokyo, Japan).

2.9. Data analysis

Independent triplicates were done in this study. The results were presented as the mean with the standard deviation. The differences ($P < 0.05$) between the tests were analyzed by Origin Pro 9.0.5 using Duncan's multiple analysis.

3. Results and discussion

3.1. Characterization of the TWIP/KC mixtures

3.1.1. Turbidity, particle size and zeta potential of the TWIP/KC mixtures

When proteins are mixed with KC, interactions occur between the proteins and KC (Sow, Chong, et al., 2018). To explore the characteristics of the TWIP/KC mixtures, the effects of KC on the appearance, turbidity, D_H and zeta potential of TWIP/KC mixtures (4.0%, w/v) were determined (Fig. 1). We observed no difference in the appearance of the different TWIP/KC mixtures (Fig. 1A). However, the turbidity of the TWIP/KC mixtures decreased with the addition of KC content and the turbidity of mixtures was lower than that of TWIPs only (Fig. 1B). The decrease in the turbidity is probably caused by the protection of sulfated polysaccharides at the hydrophobic sites of the protein against loss of solubility (Antonov & Zhuravleva, 2019). It has been reported that the charge density of KC is about 0.92 sulfate groups per disaccharide (Hugerth & Sundelöf, 2001). Besides, proteins can capture some biopolymers to produce soluble complexes in water, which do not affect the turbidity and result in the reduction in the overall turbidity of the mixture (Berino et al., 2019).

To further characterize the TWIP/KC mixtures, the particle size was determined. Dynamic light scattering was implemented on the TWIP/KC mixtures to determine the D_H of the particles in the mixtures (Sow, Toh, Wong, & Yang, 2019). The addition of KC did not affect the D_H of TWIP/KC mixtures until the mixing ratio reached 80:20 (w/w) at a fixed mixture concentration of 4.0% (v/v), as shown in Table S1. The D_H of the TWIP/KC mixtures at 80:20 (w/w) was 485.07 ± 36.90 nm, which was higher than that of the TWIPs alone (360.87 ± 11.34 nm) (Fig. 1C). The D_H of the TWIPs was in agreement with the previous report (Ren, Chen, Zhang, Lin, et al., 2019).

The TWIP/KC mixtures were negatively charged at the neutral pH, as shown in Fig. 1D. The zeta potential for both polymers was negative, confirming the strong repulsion between them (Santos, Da Costa, & Garcia-Rojas, 2018). The zeta potential of the different TWIP/KC dispersion was no significant difference ($P < 0.05$). This result was in
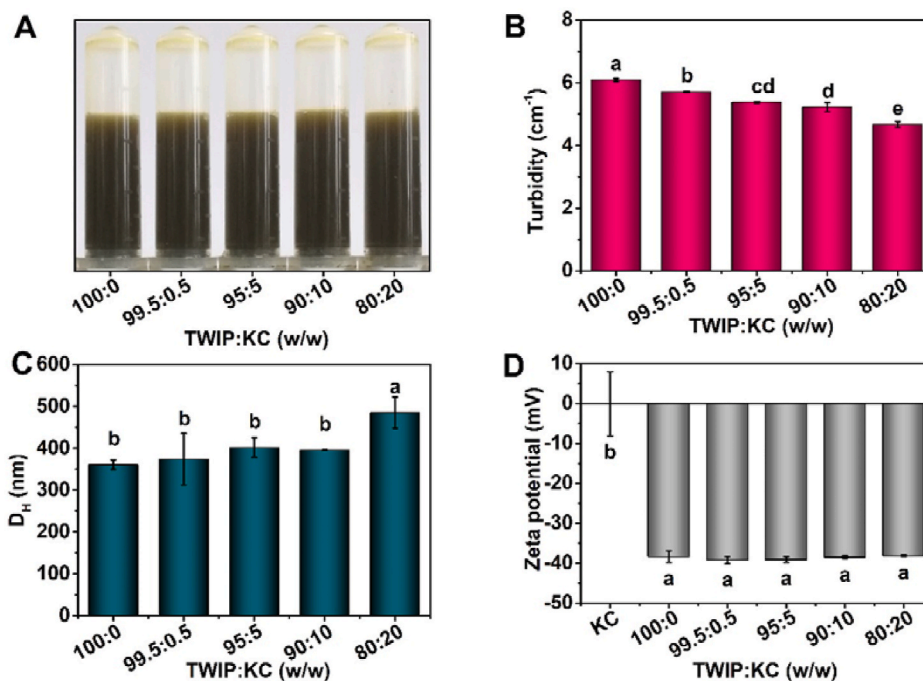

Fig. 1. Effect of the mixing of TWIPs with KC on (A) appearance of the mixtures (4.0%, w/v), (B) turbidity, (C) D_H and (D) zeta potential.
*TWIP, KC and D_H represent tea water-insoluble protein, κ-carrageenan and hydrodynamic diameter, respectively. Lowercase letters denote the difference ($P < 0.05$) among the groups.

accordance with the zeta potential value of SPI/KC mixtures which showed no change after the addition of KC (Mao et al., 2017). All the TWIP/KC mixtures were negatively charged at more than 35 mV approximately, which was equal to that of TWIP. Electrostatic repulsion resulted in the stabilization of the mixture suspension at the mixing ratios. However, sufficient KC broke through the steric exclusion to combine with the TWIPs, driving the formation of the complex aggregates of TWIP/KC mixtures. Therefore, the D_H of TWIP/KC mixtures at 80:20 increased compared with that of the other TWIP/KC mixtures (Fig. 1C).

3.1.2. Secondary structure of the TWIP/KC mixtures

The structure of the TWIPs was affected by the addition of KC. The FTIR spectra and secondary structures of the different TWIP/KC mixtures are shown in Fig. 2. Compared with the TWIPs, the characteristic peak of KC at the 847 cm^{-1} appeared in the mixtures at TWIP/KC ratios of 95:5, 90:10 and 80:20. The characteristic peaks of the TWIP/KC mixtures are shown in Table S2. The positions of the characteristic peaks were determined according to previously published methods (Ren, Chen, Zhang, Zhao, et al., 2019; Wang, Chen, An, Chang, & Song, 2018). The stretching vibration of C4–O–S appeared at 850-840 cm^{-1}, which indicates the monomer of κ-KC (Şen & Erboz, 2010). This showed that the TWIPs in the TWIP/KC mixtures might interact with KC. With the addition of KC, the peak of COO$^-$ at 1650 cm^{-1} and 1542 cm^{-1} did not shift and the peak of –OH at 3390 cm^{-1} also did not change (Fig. 2). The peak near 3390 cm^{-1} was attributed to the overlaying of –OH and –NH$_2$ stretching vibrations (Chen et al., 2020).

The secondary structures of the different TWIP/KC mixtures with the increase of KC addition are presented in Table S3. The presence of KC in the mixtures at TWIP/KC ratios of 95:5, 90:10 and 80:20 increased the number of β-sheet, α-helix and β-antiparallel. Compared with TWIPs without KC, the amount of β-turn and random coil was reduced after the addition of KC. These results indicated that the β-turn and the random coil of the TWIPs in the mixtures were transformed into β-sheet, α-helix and β-antiparallel due to the addition of KC. The partial unfolding of proteins could be beneficial for emulsification (Setia et al., 2019). These results are in line with those of the previous research about the effect of KC on whey protein structure (Alizadeh-Pasdar, Nakai, & Li-Chan, 2002). This could be attributed to the interaction between the additional KC and the TWIPs as a previous report indicates that the interaction between the fish gelatin and KC increases due to the increase of KC ratio (Sow, Chong, et al., 2018). The interaction between KC and

Fig. 2. FTIR spectra of different TWIP/KC mixtures.
*TWIP, KC and FTIR represent tea water-insoluble protein, κ-carrageenan and Fourier transform infrared, respectively.

TWIP was mainly noncovalent bonding forces like hydrophobic interaction and disulfide bonds as previous reports (Mao et al., 2017; Tavernier et al., 2017). Therefore, the addition of KC increased the probability for the interaction between TWIP and KC and intermolecular KC interaction. Furthermore, the change in secondary structure would affect the characteristics of the TWIPs such as their emulsifying property and viscoelastic behavior.

3.1.3. Morphology of the TWIP/KC mixtures

To further explore the effect of KC on the structure of TWIP/KC mixtures, the morphology of the TWIP/KC mixtures was assessed using AFM. AFM helps illustrate the TWIP aggregation behavior, which is related to their morphological characteristics (Ren, Chen, Zhang, Lin, et al., 2019). The typical AFM images of the TWP/KC mixtures are shown in Fig. 3. Compared with TWIPs without the addition of KC (Fig. 3A), the protein particles progressively clustered with the increase of KC addition, as presented in Fig. 3B–E. In particular, the TWIP/KC mixtures at a ratio of 80:20 became aggregated and clustered, resulting in an increase in D_H, as shown in Fig. 1C. As previously reported, even a low amount of KC can form networks between the KC molecules or with proteins like fish gelatin, resulting in the formation of aggregates with different morphologies such as sphere or irregular shapes (Sow, Chong, et al., 2018). The typical 3D-view of the AFM images of TWIP/KC mixtures further verified the above results (Fig. 3A'-E').

3.2. Characteristics of PEs stabilized by TWIP/KC mixtures

The TWIP/KC mixtures were used as Pickering stabilizers to produce oil-in-water (O/W) PEs with different TWIP/KC ratios (between 100:0 and 80:20 (w/w)) using high-speed homogenization combined with the ultrasonic processor. The characteristics of PEs stabilized by TWIP/KC mixtures were evaluated such as the appearance, droplet size, volume fraction, area fraction, fluorescent microscopy observation, apparent viscosity and viscoelasticity (Fig. 4).

First, the TWIP/KC mixtures could form the stable appearance of the PEs stabilized by TWIP/KC mixtures (Fig. 4A). According to previous reports, TWIP nanoparticles can stabilize PEs (Ren, Chen, Zhang, Lin, et, al. 2019; 2020). All the PEs were stable during the storage time of 60 d at 4 °C and no creaming was observed in this study. After the addition of KC, the size of the PEs stabilized by TWIP/KC mixtures became small compared with those without the addition of KC (Fig. 4B). Even a little KC could effectively reduce the $d_{4,3}$ and $d_{3,2}$ of the PEs stabilized by the TWIP/KC mixtures. The volume and area diameter distribution of the PEs stabilized by TWIP/KC mixtures confirmed the reduction in size (Fig. 4C and D). The size of emulsions stabilized by SPI/KC mixtures decreased with the addition of KC (Tavernier et al., 2017). Meanwhile, the morphological changes are shown in Fig. 4E. The reduction in the droplet size of PEs stabilized by TWIP/KC mixtures was obvious compared with those stabilized by TWIPs only.

A monomodal dimensional distribution was observed in the volume and area diameter distribution of the emulsion droplets, indicating that the droplet size of PEs stabilized by TWIP/KC mixtures was relatively homogeneous. Moreover, the d_{10}, d_{50}, d_{90} and span values have been widely used to characterize the size distribution of food materials (Sansone et al., 2011). The d_{10}, d_{50}, d_{90} and span of PEs stabilized by TWIP/KC mixtures are presented in Table 1. Lower diameters of d_{10}, d_{50}, d_{90} and the smaller span of the volume and area diameter were observed for the PEs stabilized by TWIP/KC mixtures compared with those stabilized by TWIP particles only. Taken together, these results indicated that the addition of KC reduced the droplet size of the PEs stabilized by TWIP/KC mixtures. This could be attributed to that reducing the turbidity improved the stability of the TWIP/KC mixtures by inhibiting the interaction between the different TWIP particles, which was beneficial for the formation of small emulsion droplets, thus avoiding emulsion aggregation (Ren, Chen, Zhang, Lin, et al., 2019).

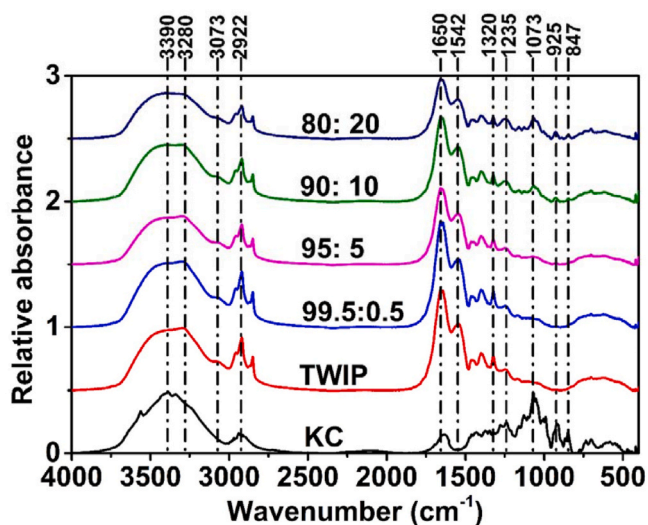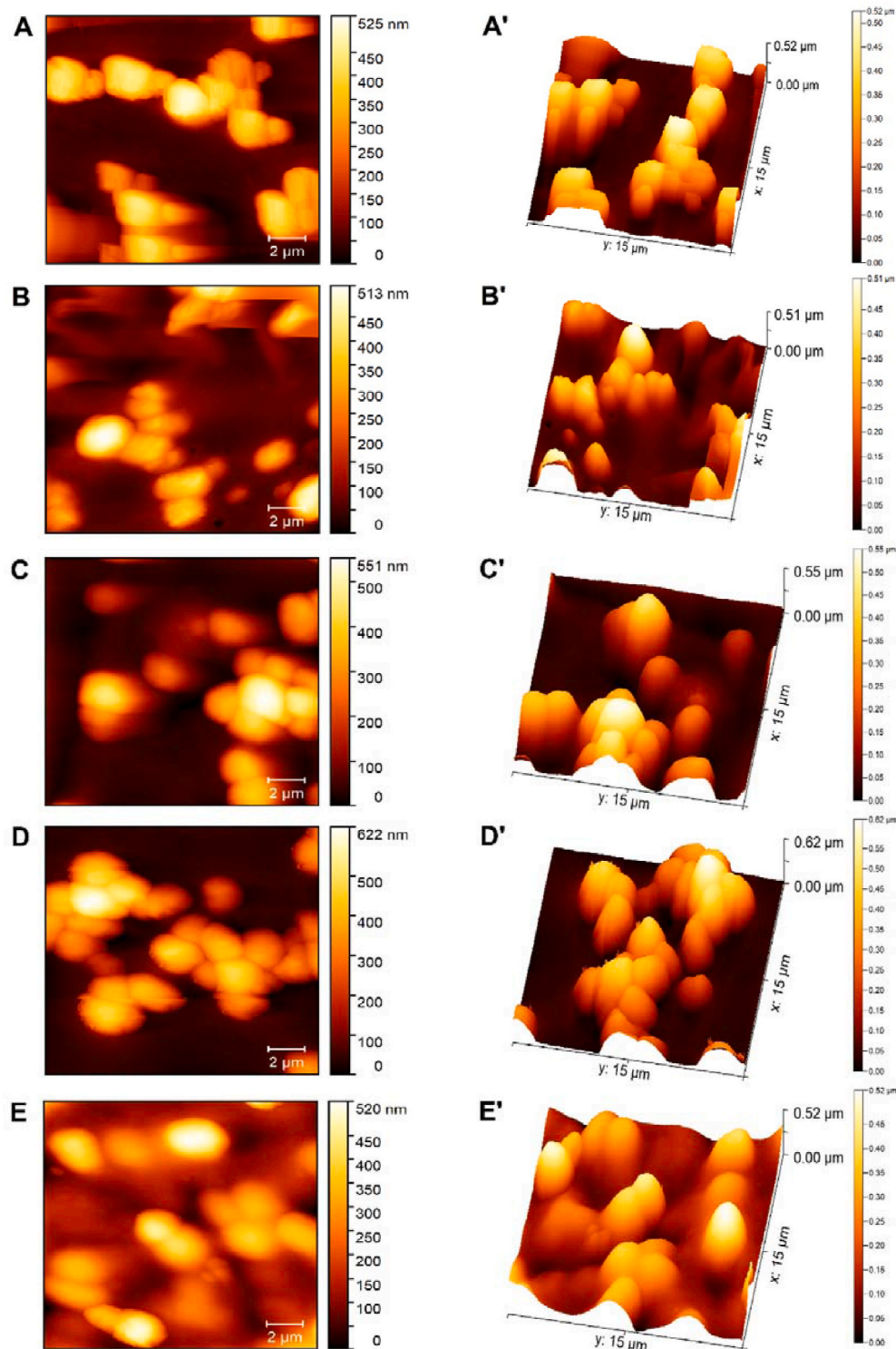Besides, wettability is one of the most important indicators for

Fig. 3. Typical atomic force microscopy (AFM) images of TWP/KC mixtures (A and A': 100:0; B and B': 99.5:0.5; C and C': 95:5; D and D': 90:10; E and E': 80:20.). *TWIP and KC represent tea water-insoluble protein and κ-carrageenan, respectively.

evaluating particles to stabilize PEs, which can be explained by contact angle (Wei, Yu, et al., 2020). After the addition of KC, the contact angle of TWIP/KC mixtures reduced and their contact angle was close to 90° at 90:10 and 80:20 (Table S4), indicating that the TWIP/KC mixtures at 90:10 and 80:20 were amphipathic to benefit for the stability of PEs. The majority of previous research indicates that reducing the size of the droplets of PEs could improve their storage stability, for example, those stabilized using soy protein nanoparticle aggregates, TWIPs, gliadin

(Liu, Liu, Guo, Yin, & Yang, 2017; Liu & Tang, 2013; Ren, Chen, Zhang, Lin, et al., 2019).

The rheological properties of PEs stabilized by proteins are important to evaluate their emulsifying properties. Therefore, the apparent viscosity of the PEs stabilized by TWIP/KC mixtures is shown in Fig. 4F. Under the low shear rate of 10 s^{-1}, the apparent viscosity of the PEs stabilized by TWIP/KC mixtures decreased sharply with the increase of the shear rate. This indicated that the PEs stabilized by TWIP/KC
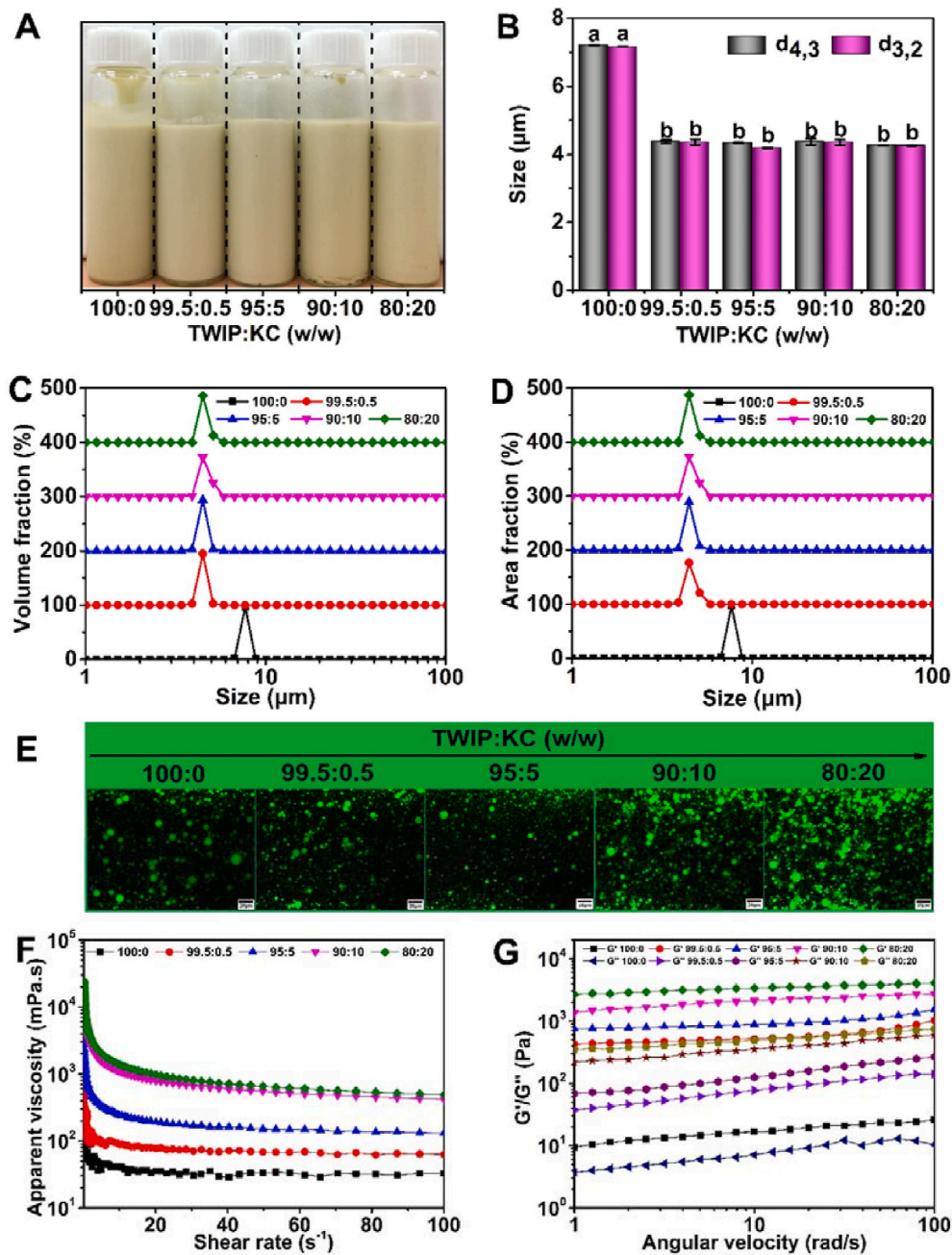
Fig. 4. Appearance (A), size (B), volume fraction (C) and area fraction (D), fluorescent microscopy observation (E), apparent viscosity (F) and viscoelasticity (G) of Pickering emulsions stabilized using TWIP/KC mixtures.
*TWIP and KC represent tea water-insoluble protein and κ-carrageenan, respectively.

Table 1
The d_{10}, d_{50}, d_{90} and span of Pickering emulsions stabilized by TWIP/KC mixtures.

TWIP/KC mixtures	Volume diameter (µm)			Span	Area diameter (µm)			Span
	d_{10}	d_{50}	d_{90}		d_{10}	d_{50}	d_{90}	
100:0	6.79 ± 0.00[a]	7.18 ± 0.00[a]	7.59 ± 0.00[a]	0.11	6.79 ± 0.00[a]	7.18 ± 0.00[a]	7.60 ± 0.00[a]	0.11
99.5:0.5	3.98 ± 0.02[b]	4.34 ± 0.08[b]	4.92 ± 0.07[b]	0.22	3.98 ± 0.02[b]	4.35 ± 0.08[b]	4.92 ± 0.08[b]	0.22
95:05	3.94 ± 0.00[c]	4.28 ± 0.01[b]	4.43 ± 0.02[c]	0.11	3.96 ± 0.00[b]	4.35 ± 0.05[b]	4.87 ± 0.05[b]	0.21
90:10	3.98 ± 0.02[b]	4.33 ± 0.10[b]	4.90 ± 0.07[b]	0.21	3.98 ± 0.02[b]	4.34 ± 0.10[b]	4.90 ± 0.07[b]	0.21
80:20	3.96 ± 0.00[b]	4.22 ± 0.01[b]	4.67 ± 0.05[c]	0.17	3.97 ± 0.00[b]	4.23 ± 0.01[b]	4.68 ± 0.05[b]	0.17

*TWIP, KC, d_{10}, d_{50} and d_{90} indicate tea water-insoluble protein, κ-carrageen and the diameter at the 10th, 50th and 90th percentile of the particle size distribution, respectively. Upper letters indicate significant differences ($P < 0.05$). Span value is calculated as $(d_{90}-d_{10})/d_{50}$.

mixtures presented approximate Newtonian fluid rheological properties (Fig. 4F). The PEs stabilized by TWIP/KC mixtures displayed shear-thinning behavior, which is a common phenomenon in fluids (Boutin, Giroux, Paquin, & Britten, 2007). The shear-thinning phenomenon has been observed for PEs stabilized by octenylsuccinate quinoa starch granules (Li et al., 2019), zein/pectin composite nanoparticles (Jiang et al., 2019) and TWIPs (Ren et al., 2020).

With the increase in shear rate, the apparent viscosity of the PEs stabilized by TWIP/KC mixtures became small and gradually stabilized. Under these conditions, the PEs stabilized by TWIP/KC mixtures were considered as a pseudoplastic fluid. This might be attributed to the fact that the protein molecules gradually move in the same direction with the increase in the shear rate and the intermolecular force decreases leading to the breakage of chemical bonds such as hydrogen bonds and the dissociation of protein molecules (Liu & Tang, 2011). The apparent viscosity of the PEs stabilized by TWIP/KC mixtures increased with the increase of KC content in the mixtures. As shown in Table 2, the apparent viscosity of the PEs stabilized by TWIP/KC mixtures significantly ($P <$ 0.05) increased with the increase of the TWIP/KC ratio at the shear rate of 100 s^{-1}. The apparent viscosity of PEs stabilized by TWIP/KC mixtures at 90:10 and 80:20 was similar. This could be because the effect of the high shear rate on the direction of the droplets is greater than the random effect caused by Brownian motion; therefore, the droplets are oriented and the viscosity tends to be fixed when the shear rate reaches a certain level (Fuller et al., 2015). Besides, KC improved the viscosity of PEs stabilized by TWIP/KC mixtures because of the thickening effect of KC (Sow, Chong, et al., 2018). In addition, the high apparent viscosity could also effectively delay the aggregation between the droplets, thus improving the stability of the PEs stabilized by TWIP/KC mixtures.

The dynamic oscillatory results of the PEs stabilized by TWIP/KC mixtures are shown in Fig. 4G. The G′ of the PEs stabilized by TWIP/KC mixtures was higher than G″ within the angular velocity range of 0.1–100 rad/s. This showed that the PEs stabilized by TWIP/KC mixtures possessed a gel-like behavior as previous reports (Li et al., 2019; Li, Fu, et al., 2020; Liu & Tang, 2016; Nazir, Asghar, & Maan, 2017; Tavernier et al., 2017). The elastic behavior of PEs stabilized by TWIP/KC mixtures was greatly improved with the increase of KC content. The G′ and G″ of the PEs stabilized by TWIP/KC mixtures increased significantly ($P < 0.05$) with the increase of TWIP/KC ratio at an angular velocity of 10 rad/s (Table 2). This might be contributed to the formation of network structure in the PEs stabilized by TWIP/KC mixtures after the addition of KC in the continuous phase during the entire scanning range. KC can improve the colloidal properties of emulsions (Jiang et al., 2019). A thick layer can be formed at the oil-water interface by TWIP/KC mixtures and the dissociative KC could generate the three-dimensional network structure between the droplets. As previously reported, TWIP nanoparticles adsorbed at the surface of the emulsion droplets can form an interfacial film at the oil-water interface (Ren, Chen, Zhang, Lin, et al., 2019). Moreover, KC can interact with proteins to generate network regions (Sow, Chong, et al., 2018).

3.3. Fish oil gels

From the previous section, TWIP/KC mixtures were able to stabilize the fish oil-in-water PEs. Many PEs were utilized to prepare oil gels like those stabilized by octenylsuccinate quinoa starch granules (Li et al., 2019) and gliadin-chitosan-complexes (Yuan et al., 2017; Zhou et al., 2019). In this study, fish oil gels were then prepared using fish oil-in-water PEs stabilized by TWIP/KC mixtures as templates. The appearance of the fish oil gels prepared using PEs stabilized by TWIP/KC mixtures is displayed in Fig. 5A. Oil overflow was observed for the fish oil gels prepared using the PEs at TWIP/KC ratios of 100:0, 99.5:0.5 and 95:5. However, the fish oil gels prepared using the PEs at TWIP/KC ratios of 90:10 and 80:20 showed no obvious oils at the surface. This result indicated that the fish oil gels prepared using the PEs at TWIP/KC ratios of 90:10 and 80:20 were stable.

The apparent viscosity and viscoelasticity of fish oil gels prepared using PEs stabilized by TWIP/KC mixtures are presented in Fig. 5B and C. The apparent viscosity of all fish oil gels decreased with the increase in shear rate (Fig. 5B), indicating that they exhibited shear-thinning behavior (Jiang et al., 2019). Additionally, the apparent viscosity of the fish oil gels prepared at different ratios of TWIP and KC increased with the increase in KC content. The apparent viscosity of the fish oil gels increased significantly ($P < 0.05$) with the increase in the TWIP/KC ratio at a shear rate of 100 s^{-1} (Table 2). Besides, the fish oil gels prepared at the TWIP/KC ratios of 95:5, 90:10 and 80:20 exhibited a greater G′ than G″ at the angular velocity range of 1–100 rad/s (Fig. 5C). Additionally, the G′ and G″ of fish oil gels increased significantly ($P < 0.05$) with the increase of TWIP/KC ratio at an angular velocity of 10 rad/s (Table 2). G′ represents the elastic behavior; whereas G″ represents the viscous behavior (Patel, Cludts, Sintang, Lesaffer, & Dewettinck, 2014; Sow, Kong, et al., 2018). These results indicated that all the fish oil gels had higher elastic behavior than viscous behavior.

The fish oil gels stabilized using the TWIP/KC mixtures had better solid-like properties compared with those stabilized using TWIPs only. This may be on account of the gradual formation of the gel network at the interface with the increase of KC content in the mixtures (Tavernier et al., 2017). The G′ was less than 2 kPa for fish oil gels prepared using PEs at TWIP/KC ratios of 100:0, 99.5:0.5 and 95:5 (Fig. 5C). This might be due to the suboptimal conformation of the TWIPs that lacked sufficient KC (Fig. 5C), resulting in a weaker film surrounding the oil droplets and no firm network formation. For the oil gels prepared using PEs at TWIP/KC ratios of 90:10 and 80:20, the G′ value of them was higher than 10 kPa and the G′ value of the oil gels prepared using PEs at a TWIP/KC ratio of 80:20 reached almost 200 kPa. When sufficient KC was added to induce the change of conformation of the TWIPs (Table S3), they could cover the surface of the oil droplets with TWIPs and form a better network than those at TWIP/KC ratios of 100:0, 99.5:0.5 and 95:5.

According to the foregoing analysis, a schematic model was proposed for the effect of KC on the formation of fish oil gels prepared using PEs stabilized by TWIP/KC mixtures (Fig. 6). The secondary structure of the TWIPs changed in the presence of KC, which was beneficial to form

Table 2
Difference of apparent viscosity and G'/G″ of PEs stabilized by TWIP/KC mixtures and fish oil gels at a certain condition.

TWIP/KC ratio (w/w)	PEs stabilized by TWIP/KC mixtures			Fish oil gels		
	G' (Pa)	G″ (Pa)	Apparent viscosity (mPa.s)	G' (Pa)	G″ (Pa)	Apparent viscosity (mPa.s)
100:0	19±3[e]	7±1[e]	32.2 ± 4.4[e]	97 ± 10[d]	194 ± 21[d]	704.3 ± 92.7[d]
99.5:0.5	526±7[d]	78±1[d]	60.1 ± 2.2[d]	136 ± 27[d]	226±3[d]	805.0 ± 133.4[cd]
95:5	864 ± 25[c]	130±8[c]	135.1 ± 10.1[c]	1549 ± 141[c]	720 ± 110[c]	1004.1 ± 161.0[bc]
90:10	2091 ± 31[b]	359 ± 12[b]	411.7 ± 26.2[b]	12,954 ± 1738[b]	2479 ± 270[b]	1455.4 ± 330.5[b]
80:20	3245 ± 188[a]	468 ± 24[a]	487.3 ± 24.7[a]	149,553 ± 18331[a]	24,332 ± 3631[a]	5576.2 ± 492.5[a]

*TWIP, KC, G′, G″ and PEs indicate tea water-insoluble protein, κ-carrageen and storage modulus, loss modulus and Pickering emulsions, respectively. Upper letters indicate significant differences ($P < 0.05$) between different TWIP/KC ratios. Apparent viscosity is the value at the shear rate of 100 s^{-1}. G′ and G″ are the value at the angular velocity of 10 rad/s.
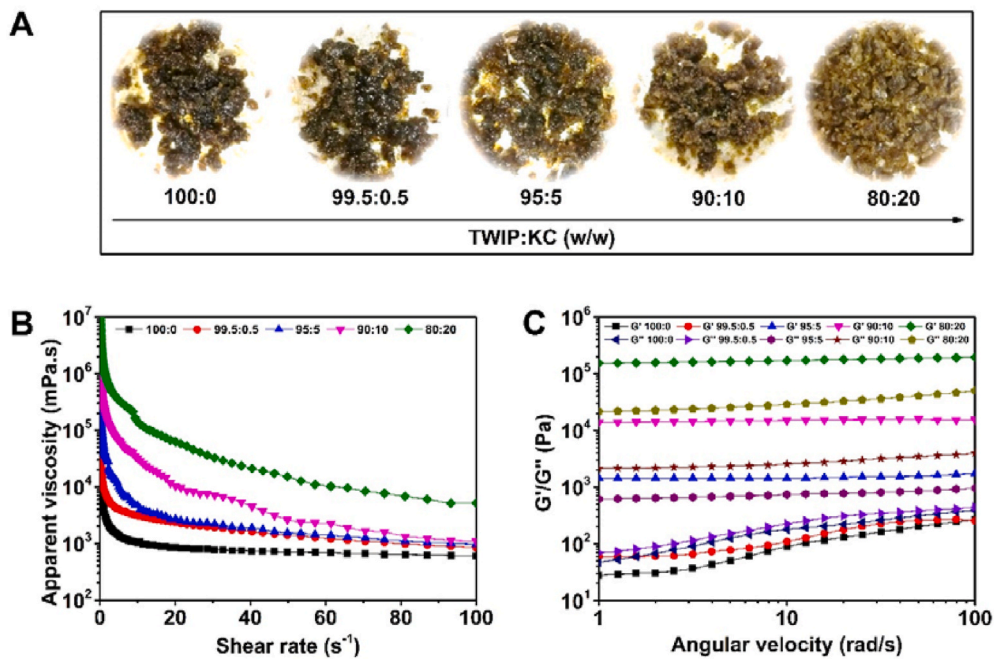
Fig. 5. Appearance (A), apparent viscosity (B) and viscoelasticity (C) of fish oil gels prepared with Pickering emulsions stabilized using TWIP/KC mixtures. *TWIP and KC represent tea water-insoluble protein and κ-carrageenan, respectively.
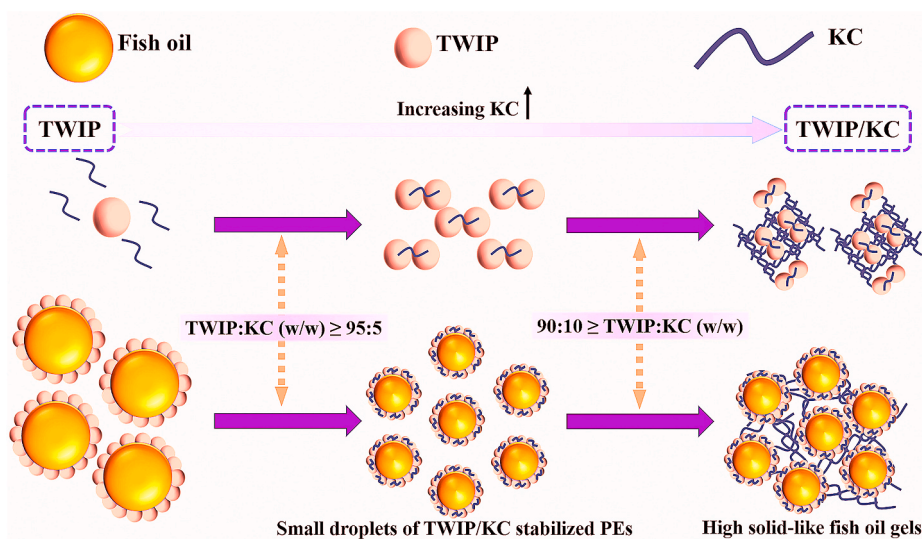

Fig. 6. Schematic model demonstrating the effect of KC on the formation of fish oil gels prepared with Pickering emulsions stabilized using TWIP/KC mixtures. *TWIP and KC represent tea water-insoluble protein and κ-carrageenan, respectively.

interfacial films and sufficient content of KC could be located between the oil droplets. After the full removal of water, the TWIP/KC mixtures at the surface of the oil droplets could interact with each other and KC could interact with the TWIPs between the different oil droplets. This was verified by fluorescent microscopy observation of the PEs stabilized by TWIP/KC mixtures (Fig. 4E). The TWIPs were located at the oil interface and oil droplets did not combine in the PEs prepared at TWIP/KC ratios of 100:0, 99.5:0.5 and 95:5. However, the oil droplets combined with each other in the PEs prepared at TWIP/KC ratios of 90:10 and 80:20 because of sufficient KC addition. The additional KC can interact with the TWIPs at the surface of the droplets and form a network structure for the formation of high solid-like fish oil gels according to the proposed schematic model.

Compared with other emulsion-templated oil gels, a high G′ of the

fish oil gels was observed (Fig. 5C). Similar to previous reports, oil gels obtained using the same approach with mixtures of gelatin and xanthan gum had a G′ of no more than 30 kPa (Patel, Rajarethinem, Cludts, Lewille, & Dewettinck, 2014). Oil gels prepared with cellulose derivatives and xanthan gum obtained a G′ of 10 kPa (Patel, Cludts, et al., 2014). The G′ of oil gels prepared using soy protein/KC complexes had a G′ of more than 40 kPa for all samples (Tavernier et al., 2017). Compared with these previous results, the fish oil gels prepared using PEs at TWIP/KC ratios of 90:10 and 80:20 showed marked solid-like behavior. The TWIP/KC-based oil gels contained a TWIP/KC content of 6.69% (w/w), which is much lower than the protein content (15%, w/w) of oil gels created by heat-induced aggregates of whey proteins (Patel, 2018). The potential applications of oil gels can be applied to encapsulate functional components, structure foods, improve the

stability of cosmetics and regard as novel functional systems in food science (Patel, Cludts, et al., 2014). However, more studies are needed because inhibiting fat oxidation of oils will broaden the application of these PE systems in actual food systems.

4. Conclusion

In the present study, PEs were prepared at a TWIP/KC mixture concentration of 4.0% (w/v) and fixed fish oil-water ratio (6:4, v/v) using high-speed homogenization combined with ultrasonic treatment. According to the physicochemical analysis and secondary structure of the TWIP/KC mixtures, the turbidity reduced significantly ($P < 0.05$), particle size showed no significant change, except for the TWIP/KC mixture at 80:20, and the zeta potential did not alter with the gradual addition of KC. Meanwhile, the β-turn and random coil of the TWIPs transformed into β-sheet, α-helix and β-antiparallel because of the addition of KC. TWIP particles progressively clustered with the increase in KC content, especially at 80:20. The droplet size of the PEs stabilized by TWIP/KC mixtures was relatively small and homogeneous, and their viscoelastic behavior improved compared with those stabilized by TWIPs. Finally, fish oil gels prepared using the PEs stabilized by TWIP/KC mixtures had a high solid-like behavior. Therefore, the TWIP/KC mixtures could be applied to prepare stable PEs and fish oil gels prepared by using PEs as templates. This will be helpful for the preparation of new edible materials, the construction of novel colloid structures of under-used food materials and their use in real food production.

Author statement

Zhongyang Ren: Methodology, Investigation, Data curation, Writing – original draft preparation., Zhanming Li: Software. Zhongzheng Chen: Writing - reviw &editing. Yuanyuan Zhang: Visualization., Xiaorong Lin: Validation., Wuyin Weng: Writing - reviw &editing. Hongshun Yang: Supervision. Bin Li: Supervision.

Declaration of competing interest

We declare that we do not have any commercial or associative interest that represents a conflict of interest in connection with the work submitted.

Acknowledgements

Appendix A. Supplementary data

Supplementary data to this article can be found online at https://doi.org/10.1016/j.foodhyd.2020.106562.

References

Akamatsu, K., Kanasugi, S., Nakao, S., & Weitz, D. A. (2015). Membrane-integrated glass capillary device for preparing small-sized water-in-oil-in-water emulsion droplets. *Langmuir, 31*, 7166–7172.

Alizadeh-Pasdar, N., Nakai, S., & Li-Chan, E. C. Y. (2002). Principal component similarity analysis of Raman spectra to study the effects of pH, heating, and κ-carrageenan on whey protein structure. *Journal of Agricultural and Food Chemistry, 50*, 6042–6052.

Antonov, Y. A., & Zhuravleva, I. L. (2019). Complexation of lysozyme with lambda carrageenan: Complex characterization and protein stability. *Food Hydrocolloids, 87*, 519–529.

Berino, R. P., Báez, G. D., Ballerini, G. A., Llopart, E. E., Busti, P. A., Moro, A., et al. (2019). Interaction of vitamin D3 with beta-lactoglobulin at high vitamin/protein ratios: Characterization of size and surface charge of nanoparticles. *Food Hydrocolloids, 90*, 182–188.

Berton-Carabin, C. C., Sagis, L., & Schroën, K. (2018). Formation, structure, and functionality of interfacial layers in food emulsions. *Annual Review of Food Science and Technology, 9*, 551–587.

Boutin, C., Giroux, H. J., Paquin, P., & Britten, M. (2007). Characterization and acid-induced gelation of butter oil emulsions produced from heated whey protein dispersions. *International Dairy Journal, 17*, 696–703.

Chang, H. W., Tan, T. B., Tan, P. Y., Abas, F., Lai, O. M., Wang, Y., et al. (2018). Microencapsulation of fish oil using thiol-modified β-lactoglobulin fibrils/chitosan complex: A study on the storage stability and in vitro release. *Food Hydrocolloids, 80*, 186–194.

Chen, Y., Li, Z., Yi, X., Kuang, H., Ding, B., Sun, W., et al. (2020). Influence of carboxymethylcellulose on the interaction between ovalbumin and tannic acid via noncovalent bonds and its effects on emulsifying properties. *LWT-Food Science and Technology, 118*, 108778.

Endo, J., & Arita, M. (2016). Cardioprotective mechanism of omega-3 polyunsaturated fatty acids. *Journal of Cardiology, 67*, 22–27.

Fuller, G. T., Considine, T., Golding, M., Matia-Merino, L., MacGibbon, A., & Gillies, G. (2015). Aggregation behavior of partially crystalline oil-in-water emulsions: Part I-characterization under steady shear. *Food Hydrocolloids, 43*, 521–528.

Gao, Z., Yang, X., Wu, N., Wang, L., Wang, J., Guo, J., et al. (2014). Protein-based Pickering emulsion and oil gel prepared by complexes of zein colloidal particles and stearate. *Journal of Agricultural and Food Chemistry, 62*, 2672–2678.

Hugerth, A., & Sundelöf, L. (2001). The effect of polyelectrolyte counterion specificity, charge density, and conformation on polyelectrolyte-amphiphile interaction: The carrageenan/furcellaran-amitriptyline system. *Biopolymers, 58*, 186–194.

Jiang, Y., Zhang, C., Yuan, J., Wu, Y., Li, F., Li, D., et al. (2019). Effects of pectin polydispersity on zein/pectin composite nanoparticles (ZAPs) as high internal-phase Pickering emulsion stabilizers. *Carbohydrate Polymers, 219*, 77–86.

Li, K., Fu, L., Zhao, Y., Xue, S., Wang, P., Xu, X., et al. (2020). Use of high-intensity ultrasound to improve emulsifying properties of chicken myofibrillar protein and enhance the rheological properties and stability of the emulsion. *Food Hydrocolloids, 98*, 105275.

Linke, C., & Drusch, S. (2018). Pickering emulsions in foods-opportunities and limitations. *Critical Reviews in Food Science and Nutrition, 58*, 1971–1985.

Liu, X., Liu, Y., Guo, J., Yin, S., & Yang, X. (2017). Microfluidization initiated cross-linking of gliadin particles for structured algal oil emulsions. *Food Hydrocolloids, 73*, 153–161.

Liu, F., & Tang, C. H. (2011). Cold, gel-like whey protein emulsions by microfluidisation emulsification: Rheological properties and microstructures. *Food Chemistry, 127*, 1641–1647.

Liu, F., & Tang, C. H. (2013). Soy protein nanoparticle aggregates as Pickering stabilizers for oil-in-water emulsions. *Journal of Agricultural and Food Chemistry, 61*, 8888–8898.

Liu, F., & Tang, C. H. (2016). Soy glycinin as food-grade Pickering stabilizers: Part III. Fabrication of gel-like emulsions and their potential as sustained-release delivery systems for β-carotene. *Food Hydrocolloids, 60*, 631–640.

Li, Y., Zeng, Q., Liu, G., Chen, X., Zhu, Y., Liu, H., et al. (2020). Food-grade emulsions stabilized by marine Antarctic krill (*Euphausia superba*) proteins with long-term physico-chemical stability. *LWT-Food Science and Technology, 128*, 109492.

Li, S., Zhang, B., Tan, C. P., Li, C., Fu, X., & Huang, Q. (2019). Octenylsuccinate quinoa starch granule-stabilized Pickering emulsion gels: Preparation, microstructure and gelling mechanism. *Food Hydrocolloids, 91*, 40–47.

Mao, L., Wang, W., Tai, K., Yuan, F., & Gao, Y. (2017). Development of a soy protein isolate-carrageenan-quercetagetin non-covalent complex for the stabilization of β-carotene emulsions. *Food & Function, 8*, 4356–4363.

Marefati, A., Bertrand, M., Sjöö, M., Dejmek, P., & Rayner, M. (2017). Storage and digestion stability of encapsulated curcumin in emulsions based on starch granule Pickering stabilization. *Food Hydrocolloids, 63*, 309–320.

Nazir, A., Asghar, A., & Maan, A. (2017). Food gels: Gelling process and new applications. In J. Ahmed, P. Ptaszek, & S. Basu (Eds.), *Advances in food rheology and its applications* (pp. 335–353). Cambridge: Woodhead Publishing.

Nečas, D., & Klapetek, P. (2012). Gwyddion: An open-source software for SPM data analysis. *Open Physics, 10*, 181–188.

Patel, A. R. (2018). Functional and engineered colloids from edible materials for emerging applications in designing the food of the future. *Advanced Functional Materials*, 1806809.

Patel, A. R., Cludts, N., Sintang, M. D. B., Lesaffer, A., & Dewettinck, K. (2014). Edible oleogels based on water soluble food polymers: Preparation, characterization and potential application. *Food and Function, 5*, 2673–3028.

Patel, A. R., Rajarethinem, P. S., Cludts, N., Lewille, B., & Dewettinck, K. (2014). Biopolymer-based structuring of liquid oil into soft solids and oleogels using water-continuous emulsions as templates. *Langmuir, 31*, 2065–2073.

Ren, Z., Chen, Z., Zhang, Y., Lin, X., & Li, B. (2019). Novel food-grade Pickering emulsions stabilized by tea water-insoluble protein nanoparticles from tea residues. *Food Hydrocolloids, 96*, 322–330.

Ren, Z., Chen, Z., Zhang, Y., Lin, X., & Li, B. (2020). Characteristics and rheological behavior of Pickering emulsions stabilized by tea water-insoluble protein nanoparticles via high-pressure homogenization. *International Journal of Biological Macromolecules, 151*, 247–256.

Ren, Z., Chen, Z., Zhang, Y., Zhao, T., Ye, X., Gao, X., et al. (2019). Functional properties and structural profiles of water-insoluble proteins from three types of tea residues. *LWT-Food Science and Technology, 110*, 324–331.

Sansone, F., Mencherini, T., Picerno, P., D'Amore, M., Aquino, R. P., & Lauro, M. R. (2011). Maltodextrin/pectin microparticles by spray drying as carrier for nutraceutical extracts. *Journal of Food Engineering, 105*, 468–476.

Santos, M. B., Da Costa, N. R., & Garcia-Rojas, E. E. (2018). Interpolymeric complexes formed between whey proteins and biopolymers: Delivery systems of bioactive ingredients. *Comprehensive Reviews in Food Science and Food Safety, 17*, 792–805.

Selig, M. J., Dar, B. N., Kierulf, A., Ravanfar, R., Rizvi, S. S. H., & Abbaspourrad, A. (2018). Modulation of whey protein-kappa carrageenan hydrogel properties via enzymatic protein modification. *Food and Function, 9*, 2313–2319.

Şen, M., & Erboz, E. N. (2010). Determination of critical gelation conditions of κ-carrageenan by viscosimetric and FT-IR analyses. *Food Research International, 43*, 1361–1364.

Setia, R., Dai, Z., Nickerson, M. T., Sopiwnyk, E., Malcolmson, L., & Ai, Y. (2019). Impacts of short-term germination on the chemical compositions, technological characteristics and nutritional quality of yellow pea and faba bean flours. *Food Research International, 122*, 263–272.

Souza, R. J. D., Mente, A., Maroleanu, A., Cozma, A. I., Ha, V., Kishibe, T., et al. (2015). Intake of saturated and trans unsaturated fatty acids and risk of all cause mortality, cardiovascular disease, and type 2 diabetes: Systematic review and meta-analysis of observational studies. *British Medical Journal, 351*, h3978.

Sow, L. C., Chong, J. M. N., Xu, L., & Yang, H. (2018). Effects of κ-carrageenan on the structure and rheological properties of fish gelatin. *Journal of Food Engineering, 239*, 92–103.

Sow, L. C., Kong, K., & Yang, H. (2018). Structural modification of fish gelatin by the addition of gellan, κ-carrageenan, and salts mimics the critical physicochemical properties of pork gelatin. *Journal of Food Science, 83*, 1280–1291.

Sow, L. C., Tan, S. J., & Yang, H. (2019). Rheological properties and structure modification in liquid and gel of tilapia skin gelatin by the addition of low acyl gellan. *Food Hydrocolloids, 90*, 9–18.

Sow, L. C., Toh, N. Z. Y., Wong, C. W., & Yang, H. (2019). Combination of sodium alginate with tilapia fish gelatin for improved texture properties and nanostructure modification. *Food Hydrocolloids, 94*, 459–467.

Tavernier, I., Heyman, B., Van der Meeren, P., Ruyssen, T., & Dewettinck, K. (2019). Oil powders stabilized with soy protein used to prepare oil-in-fat dispersions. *Journal of Food Engineering, 244*, 136–141.

Tavernier, I., Patel, A. R., Van der Meeren, P., & Dewettinck, K. (2017). Emulsion-templated liquid oil structuring with soy protein and soy protein: κ-Carrageenan complexes. *Food Hydrocolloids, 65*, 107–120.

Wang, Y., Chen, L., An, F., Chang, M., & Song, H. (2018). A novel polysaccharide gel bead enabled oral enzyme delivery with sustained release in small intestine. *Food Hydrocolloids, 84*, 68–74.

Wang, L., Yin, S., Wu, L., Qi, J., Guo, J., & Yang, X. (2016). Fabrication and characterization of Pickering emulsions and oil gels stabilized by highly charged zein/chitosan complex particles (ZCCPs). *Food Chemistry, 213*, 462–469.

Wei, Y., Sun, C., Dai, L., Mao, L., Yuan, F., & Gao, Y. (2019). Novel bilayer emulsions costabilized by zein colloidal particles and propylene glycol alginate, Part 1: Fabrication and characterization. *Journal of Agricultural and Food Chemistry, 67*, 1197–1208.

Wei, Y., Tong, Z., Dai, L., Wang, D., Lv, P., Liu, J., et al. (2020). Influence of interfacial compositions on the microstructure, physiochemical stability, lipid digestion and β-carotene bioaccessibility of Pickering emulsions. *Food Hydrocolloids, 104*, 105738.

Wei, Y., Yu, Z., Lin, K., Yang, S., Tai, K., Liu, J., et al. (2020). Fabrication, physicochemical stability, and microstructure of coenzyme Q10 Pickering emulsions stabilized by resveratrol-loaded composite nanoparticles. *Journal of Agricultural and Food Chemistry, 68*, 1405–1418.

Xiao, J., Li, Y., & Huang, Q. (2016). Recent advances on food-grade particles stabilized Pickering emulsions: Fabrication, characterization and research trends. *Trends in Food Science & Technology, 55*, 48–60.

Yuan, D., Hu, Y., Zeng, T., Yin, S. W., Tang, C., & Yang, X. (2017). Development of stable Pickering emulsions/oil powders and Pickering HIPEs stabilized by gliadin/chitosan complex particles. *Food & Function, 8*, 2220–2230.

Zhou, Y., & Yang, H. (2019). Effects of calcium ion on gel properties and gelation of tilapia (*Oreochromis niloticus*) protein isolates processed with pH shift method. *Food Chemistry, 277*, 327–335.

Zhou, F., Yu, X., Zeng, T., Yin, S., Tang, C., & Yang, X. (2019). Fabrication and characterization of novel water-insoluble protein porous materials derived from Pickering high internal-phase emulsions stabilized by gliadin-chitosan-complex particles. *Journal of Agricultural and Food Chemistry, 67*, 3423–3431.